Analysis and Calibration of System Errors in Steerable Parametric Loudspeakers

Chuang Shi and Woon-Seng Gan

School of Electrical and Electronic Engineering,

Nanyang Technological University, Singapore

(e-mail: shichuang@e.ntu.edu.sg; ewsgan@ntu.edu.sg)

Abstract

By adjusting a set of delay amounts and amplitudes of the ultrasonic transducer (primary source) array in parametric loudspeakers, the directional sound beam can be steered within a range of predefined angles. This beamsteering characteristic of parametric loudspeakers has been proposed in theory and validated by measurements. In particular, the locations of the mainlobe and grating lobes can be predicted within a certain degree of accuracy in theory. However, errors incur in different stages of implementation. Thus, mismatches are observed between theoretical and measured beampatterns. In this paper, four types of system errors are analyzed for the primary-frequency waves and the difference-frequency waves based on the phased array theory and the product directivity principle, respectively. The degraded beampatterns which are caused by system errors are analyzed and calibrated by using a combined optimization approach of Monte Carlo method and nonlinear least squares method. Experimental results are presented to show the advantage of the proposed calibration method that leads to significant reduction of mismatch between theoretical and measured beampatterns at both the primary frequency and the difference frequency.

Keywords: *parametric acoustic array, ultrasonic transducer, array calibration, Monte Carlo method*.

1. Introduction

The theoretical explanation of parametric array effect can be traced back to Westervelt's work [1] in 1963. He investigated the generation of low-frequency wave (also known as the difference-frequency wave) through underwater interaction of high-frequency waves (also known as the primary-frequency waves). It is not until 1975 when Bennett and Blackstock [2] first validated the existence of parametric array effect in air. In 1983, Yoneyama et al. [3] developed the first parametric array loudspeaker that was able to create so-called "audio spotlight" by amplitude modulating a high intensity ultrasonic carrier signal with audible signal. More recently, various techniques are developed to achieve a controllable audio beam [4]. Olszewski et al. [5] built a hybrid system to turn the sound beam mechanically in large angular step size and electrically in small angular step size. However, the drawback of this hybrid system is its bulky mechanical structure and unavoidable reflections caused by louvers in the system. The digital beamsteering approach was proposed by Gan et al. [6]. The difference-frequency beampattern (i.e. audible sound beam) is controlled by adjusting the primary-frequency beampatterns electronically in a delay-and-sum beamforming structure. Tanaka et al. [7] utilized steerable parametric loudspeakers in the active noise control application that is able to send an anti-noise sound wave towards a tracked moving target.

The basis of this beamsteering capability is the theoretical study of scattering of sound by sound carried out by Darvennes and Hamilton [8]. They show that the difference-frequency wave is generated from two non-collinear primary Gaussian beams based on the nonlinear parabolic wave equation. When the Gaussian beams are restricted to moderate source separations and interaction angles, the far-field difference-frequency directivity is given by the product of the primary-frequency directivities. However, the early measurements obtained by Muir and Willette

[9] shows that the absence of sidelobes and a rather wide beamwidth in the difference-frequency directivity. It is the sum-frequency beam that is narrower than the primary-frequency mainlobe and can be predicted by the product directivity principle approximately. Similar observations are also made from the results presented by the authors [10]. The linear ultrasonic transducer array is transformed to an equivalent Gaussian source array in order to fulfill the prerequisites of the product directivity principle. The steerable parametric loudspeaker, as well as the grating lobe elimination, is verified to be feasible through experimental measurements. However, there are certain discrepancies between the measured directivities and the theoretical beampatterns at the primary frequency, and the mismatch problem became more critical when the difference-frequency beampatterns obtained by measurement is compared with the product of the primary-frequency beampatterns.

In this paper, we analyze and calibrate the errors in steerable parametric loudspeakers in order to solve the problem of mismatch between theoretical and measured beampatterns at the primary frequency. The cause of mismatch in the primary-frequency beampattern is mainly due to the frequency characteristic of the piezoelectric ceramic actuator. Hence, a beamsteering structure is proposed to incorporate spacing error, weight error, delay error, and channel directivity. The performance of steerable parametric loudspeakers in terms of the normalized amplitude of the grating lobe at the difference frequency are numerically analyzed under the assumptions of four types of system errors and the product directivity principle. Furthermore, the product directivity principle partially contributes to the mismatch in the difference-frequency beampatterns. Based on previous observation in measurements [9, 10], since only the local peak values achieve good agreement between theory and measurement at the difference frequency, it is suggested to use the envelope of the product of the primary-frequency beampatterns to predict

the difference-frequency beampattern. A combined optimization approach of Monte Carlo method and nonlinear least squares method is employed to calibrate steerable parametric loudspeakers based on measured primary-frequency beampatterns. The comparisons between measured and calibrated beampatterns are conducted. The reductions in mismatches of measured and theoretical beampatterns at both the primary frequencies and the difference frequencies prove the effectiveness of our proposed calibration method.

This paper is organized as follows. The proposed beamsteering structure and the analysis of system errors are presented in Section 2. It is followed by the description of the calibration algorithm for steerable parametric loudspeakers in Section 3. In Section 4, the measurement results are shown and calibration data are listed. Significant improvements in matching the theoretical and measured beampatterns are observed through the comparison between before and after calibration. Section 5 concludes the main findings in this paper.

2. Analysis of system errors in parametric loudspeakers

Based on the analysis derived by Darvennes and Hamilton [8], the sound field generated by two Gaussian beams consists of scattered wave and pumped wave. The scattered wave is generated entirely in the near-field and cannot be ignored until hundreds of Rayleigh distances. But the pumped wave continuously receives energy from the primary-frequency waves, and its beampattern depends only on the product directivity of the two Gaussian beams. In the applications of steerable parametric loudspeakers [4], the listeners are expected to be few meters away from the ultrasonic transducer, which is usually close to the Rayleigh distance and the absorption distance. In this case, the scattered wave is generated and forms the sound field together with the pumped wave. Thus, the product directivity principle may not be used simply to approximate the difference-frequency beampattern generated from the two Gaussian beams

and furthermore the ultrasonic transducer array in parametric loudspeakers. It is noted by Berntsen et al. [11] that scattered sum-frequency wave is to be found in the angular region delimited by the axis of the primary-frequency beams, but the scattered difference-frequency wave is to be found outside that region. When the scattered wave cannot be well separated from the pumped wave, a broader mainlobe at the difference frequency is expected. This explanation coincides with the measurement obtained by Muir and Willette [9] and the authors [10]. The local peak values (amplitude of the mainlobe, grating lobe and sidelobes) derived by the product directivity principle still achieve good agreement with the experimental values in above measurements. The reason is mainly due to the pumped wave that plays a dominating role on the axis of the primary-frequency beams. However, those angular region outside the local peaks may not be accurately predicted by the product directivity principle. The measured difference-frequency beampatterns shows up as monotonic when outside the local peaks. It is likely resulted from the co-existence of the pumped wave and the scattered wave. Hence, we suggest to use the envelope of the product of the primary-frequency beampatterns to predict the difference-frequency beampattern. Referring to this modified product directivity principle, the difference-frequency beampattern can still be controlled by adjusting primary-frequency beampatterns.

A fundamental structure of the beamsteerer used in steerable parametric loudspeakers is shown in Fig. 1. The total number of channels is denoted as M. According to phased array theory, the increment of delays between adjacent channels can be computed from

$$\Delta\tau = \frac{d}{c}\sin\theta_0, \tag{1}$$

where d is the spacing between channels in the ultrasonic transducer array; c is the sound speed; and θ_0 is the steering angle of the ultrasonic transducer array. Assume that the ultrasonic

transducer array is steered to the same direction θ_0 and shares the same group of weights ($w_0, w_1, \cdots, w_{M-1}$) for the primary-frequency waves. Therefore, the steering angle of the difference-frequency wave is given by the direction θ_0.

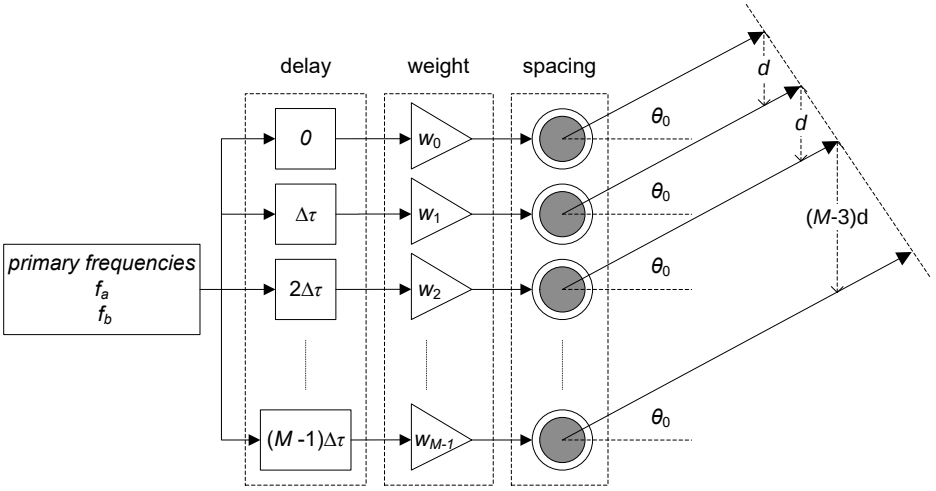

Figure 1. Beamsteering structure of steerable parametric loudspeakers based on phased array technique.

The primary-frequency beampattern in this steerable ultrasonic transducer array is given by

$$H(k,\theta) = \sum_{m=0}^{M-1} w_m \exp\left[jmdk\left(\sin\theta - \sin\theta_0\right)\right], \tag{2}$$

where w_m are the weights of channels for $m = 0,1,\cdots,M-1$; k is the wavenumber of the transmitted primary-frequency wave; θ is the incidence angle that ranges from -40˚ to 40˚ in practical application due to the beamwidth of the ultrasonic transducer [12, 13].

Based on the product directivity principle, the difference-frequency beampattern $D_{diff}(\theta)$ is given by

$$D_{diff}(\theta) = H(k_a,\theta)H(k_b,\theta), \tag{3}$$

where k_a and k_b are the wavenumbers of primary frequencies f_a and f_b, respectively. We always assume that $f_a < f_b$, without lost of generality. Thus, the difference frequency generated from the two primary-frequency waves is given by $f_{diff} = f_b - f_a$.

2.1 Conventional Array Errors

However, there are practical uncertainties in the positions of the ultrasonic transducers that may change the array configuration from the assumed uniformly distributed array. The weight (or gain) and the delay (or phase) applied to the ultrasonic transducer array may deviate from their designed ideal values due to the environmental conditions and the electro-acoustic character of the transducers [12]. Because the transducer's characteristics vary individually, it becomes impractical to calibrate steerable parametric loudspeakers by examining each single transducer in the array. The proposed calibration method in this paper categorizes the possible system errors into four types related to spacing, weight, delay, and channel directivity. The system errors are analyzed in a modified beamsteering structure, as shown in Fig. 2, where d_i is the spacing between channels, which includes the spacing errors; $\hat{w}_i$ is the distorted weight of the ith channel; τ_i is the distorted delay amount of the ith channel, $i = 0,1,\cdots,M-1$.

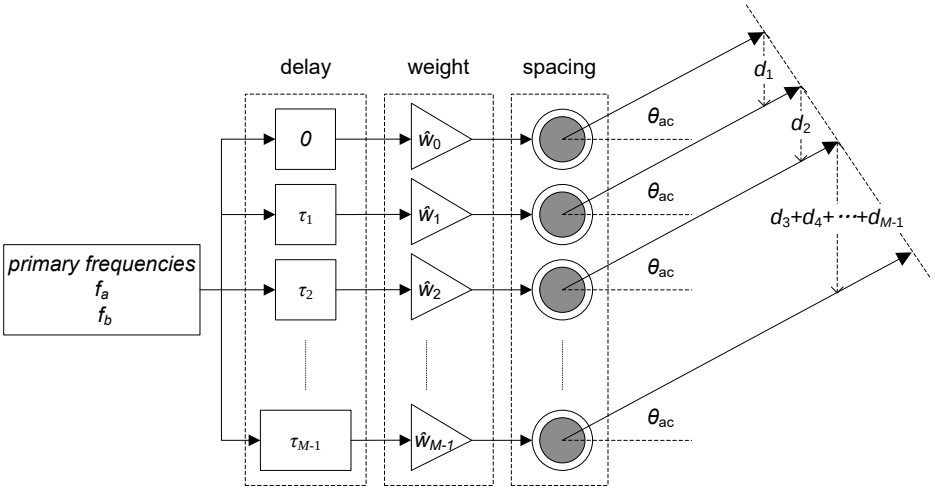

Figure 2. Proposed beamsteering structure of steerable parametric loudspeakers taking system errors into account.

It is also useful to note that the spacing error, weight error and delay error are not unique problems in parametric loudspeakers, but are also commonly found in sensor and transducer arrays. There are several conventional array calibration techniques developed for antenna arrays to solve these errors [12]. However, because system errors in parametric loudspeakers distort the primary-frequency beampattern and the subsequent difference-frequency beampattern, analytical expression to the distortion of the difference-frequency beampattern is difficult to obtain. In order to investigate this special problem, numerical simulation cases are carried out to show the amplitudes of grating lobe under different environments. The following parametric loudspeaker configurations are used in the simulations: (i) 8-channel ultrasonic transducer array; (ii) element spacing of 1 cm; (iii) emitter's center frequency of 40 kHz; (iv) using symmetric primary frequencies with reference to the center frequency. We also assume all the other conditions are ideal. Only one type of system errors is considered in each simulation case. The simulated errors are randomly generated based on normal distribution with zero mean, and the variance is decided by the limitations of the errors according to the empirical rule. The simulation results are plotted in Fig. 3 for different degrees of spacing errors, weight errors, and delay errors.

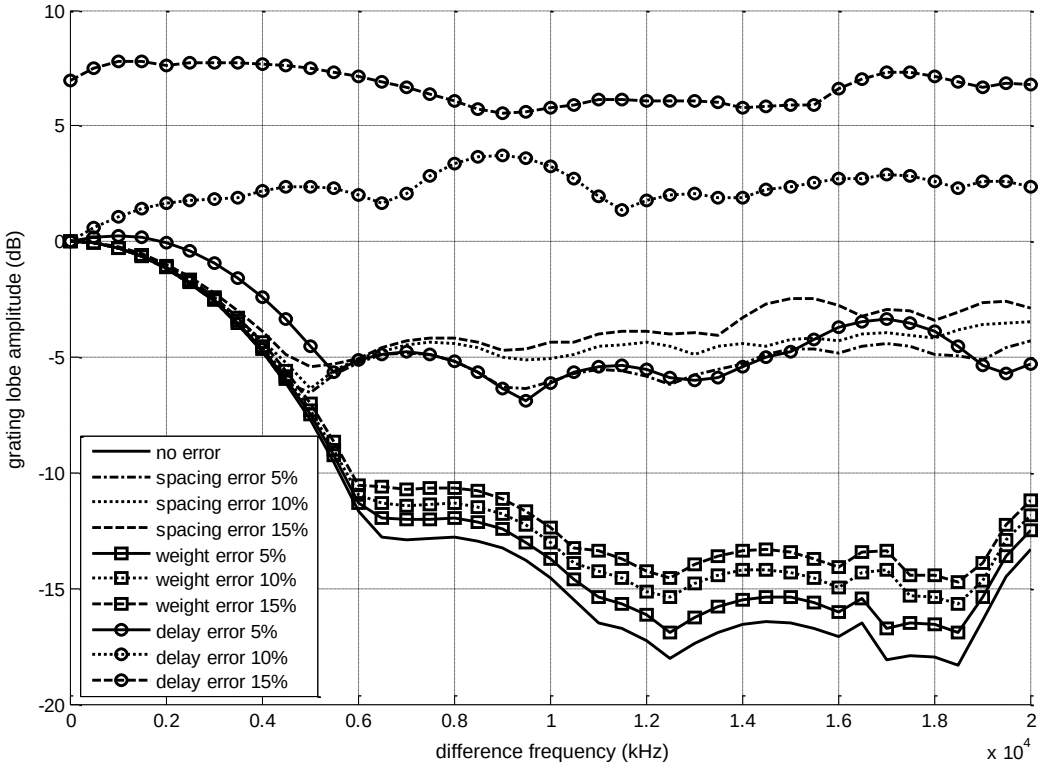

Figure 3. Effects of system errors on the spatial-aliasing performance of steerable parametric loudspeakers with 8 channel and channel spacing of 1cm.

Grating lobe elimination occurs because of the angular distance between the grating lobes of the two primary-frequency waves. When the difference frequency is small, the grating lobes of the primary-frequency waves are not far apart in term of angular distance. In this case, partial grating lobe elimination is observed. When the difference frequency is large, the angular distance of the grating lobes of the primary-frequency waves are sufficiently large, which results in grating lobe elimination [10]. In Fig. 3, when the spacing error limitation increases, the grating lobe elimination effect is significantly weakened. In contrast, the grating lobe elimination is robust to the weights errors. This is because that the weight errors mainly change the amplitudes of the sidelobes of the primary-frequency waves, while the spacing errors affect the locations of the grating lobes, which are critical to the occurrence of grating lobe elimination. The delay

error degrades the grating lobe elimination as much as the spacing error. In the case that the limitation of the delay errors is set to 10% and 15%, it is possible for the grating lobe to achieve higher amplitude than the mainlobe at certain difference frequencies.

2.2 Steering Angle Error

When we consider the primary-frequency beampattern in practice, the typical bell-shaped transducers' directivity can be considered as an additional spatial filter. This additional spatial filter results in a steering angle error in both the primary-frequency beampattern and the difference-frequency beampattern. The steering angle error is the difference between the desired steering angle and the actual steering angle, which is derived from theoretical equations and observed in simulation results. To simplify the analysis, we assume that the directivities of ultrasonic transducers are uniform with Gaussian shading [8]. The closed-form far-field directivity of Gaussian sources can be derived from the linear solution of a finite amplitude sound beam by using quasilinear theory [8], written as

$$D_G(\theta) = \exp\left[-\frac{1}{4}(ka)^2 \tan^2\theta\right], \tag{4}$$

where θ is the angle with respect to the axis of the beam, a is the effective radius of the Gaussian source, and k is the wavenumber of the operating frequency. It is noted from (4) that larger values of ka (i.e. larger ratios of source dimension to radiation wavelength) produce narrower beams. The Gaussian directivity gets shaper with higher operating frequency and larger effective radius.

Therefore, according to the product directivity principle, the difference-frequency beampattern can be computed by the product of four terms as follows:

$$D_{diff}(\theta) = D_G(k_a,\theta) H(k_a,\theta) D_G(k_b,\theta) H(k_b,\theta), \tag{5}$$

where $D_G(k,\theta)$ is the Gaussian directivity, given by (4); $H(k,\theta)$ is the primary-frequency beampattern, given by (2).

To obtain the actual steering angle, we need to find out the location of nulls for the derivative of the difference-frequency beampattern with respect to θ near the expected steering angle. Since the steering angle error is relatively small, it is approximated that the amplitude of the primary-frequency beampattern at the actual steering angle θ_{ac} is close to the amplitude at the expected steering angle, i.e. $H(k,\theta_{ac}) \approx H(k,\theta_0)$. Furthermore, assume that the weights added to each transducer are equal, and the number of transducers M is even. By substituting these approximations and (4) into the derivative of (5), we obtain

$$\frac{\partial D_{diff}(\theta)}{\partial \theta} \cong \exp\left(-\frac{k_a^2+k_b^2}{4}a^2\tan^2\theta\right)\left[\frac{\partial H(k_a,\theta)}{\partial\theta}+\frac{\partial H(k_b,\theta)}{\partial\theta}-\frac{k_a^2+k_b^2}{2}a^2\tan\theta\sec^2\theta\right]. \quad (6)$$

Because $\sin\varphi \approx \varphi$ for arbitrary small angle φ and the steering angle error is relatively small, i.e. $\sin\theta_{ac}-\sin\theta_0 \approx 0$, the derivative of the primary-frequency beampattern with respect to θ is simplified to

$$\frac{\partial H(k,\theta)}{\partial\theta} = -2\sum_{m=1}^{\frac{M}{2}}\left[\left(m-\frac{1}{2}\right)^2 k^2 d^2\cos\theta\left(\sin\theta-\sin\theta_0\right)\right]. \quad (7)$$

Substituting (7) into (6), and set the right-hand side of (6) to zero. The implicit formula for estimating the actual steering angle θ_{ac} is obtained as

$$\sin\theta_0 = \sin\theta_{ac}\left(1+\frac{6a^2}{\left(M^3-M\right)d^2\cos^4\theta_{ac}}\right). \quad (8)$$

Frequency-invariant feature of steering angle error (i.e. $\theta_{ac} - \theta_0$) is observed due to the absence of wavenumber term in (8). It is also observed in (8) that the steering angle error increases (i) when fewer transducers are used in parametric loudspeakers; (ii) when the absolute value of the steering angle increases; (iii) when the directivities of ultrasonic transducers are relatively sharper (i.e. effective radius of the transducer increases).

The steering angle errors are simulated and plotted in Fig. 4 for different numbers of transducers. Equal weights are added to the ultrasonic transducer array. The spacing is 1 cm, and the effective radius of transducer is 2.5 mm that gives a 3dB-beamwidth of 65^o at 40 kHz. In particular, when there are 4 channels in the transducer array and the expected steering angle is 20˚, the steering angle error is estimated as 0.64˚, which corresponds to a constant of 3.15% delay error to each channel in the parametric loudspeaker. Even when 8 channels are used in a compact configuration of transducer array [14], of which the spacing is half centimeter, the steering angle error is estimated to be 0.61˚ corresponding to a constant of 3% delay error to each channel for the expected steering angle of 20˚.

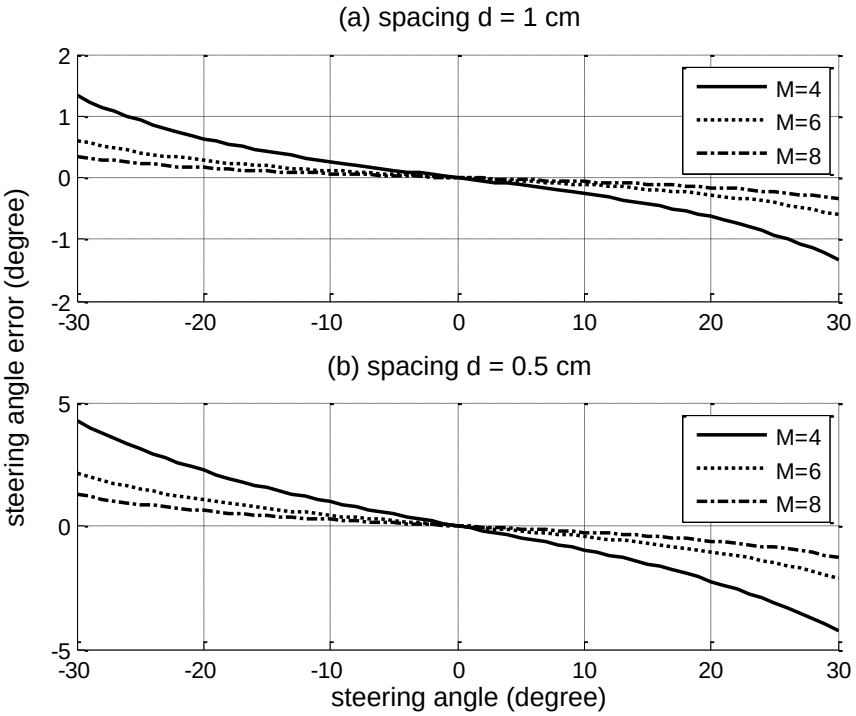

Figure 4. Steering angle errors for number of transducers M = 4, 6, 8 in a transducer array equally weighted and with channel spacing of 1 cm.

3. Calibration method for steerable parametric loudspeakers

The calibration of steerable parametric loudspeakers is based on the beamsteering structure, as shown in Fig.2. In this proposed structure, the primary-frequency beampattern is given by

$$\tilde{H}\left(k,\theta\right)=\sum_{m=0}^{M-1}\delta_W^m w_m \exp\left[\, j\delta_D^m mdk\left(\sin\theta-\delta_P^m\sin\theta_0\right)\right], \tag{9}$$

where δ_W^m is the weight distortion factor, representing the distortion of weight for the m th channel. The weight of each channel is given by $\tilde{w}_m=\delta_W^m w_m$. δ_D^m is the spacing distortion factor, representing the distortion of spacing for the m th channel. The spacing between neighboring channels is given by $d_m=\delta_D^m md$. δ_P^m is the delay distortion factor for the m th channel. Hence, the distorted delay amount of the m th channel is given by

$$\tau_m = \frac{\delta_D^m md}{c}\delta_P^m \sin\theta_0. \tag{10}$$

In (9), there are $3M$ unknown factors. The unknown distortion factors are estimated by minimizing the overall distortion between the measured directivity H_M with the distorted beampattern of the primary-frequency wave given by (9). This procedure can be described as

$$\left[\delta_W^m, \delta_D^m, \delta_P^m\right] = \arg\min \sum_{\theta} \left| H_M\left(k,\theta\right) - \tilde{H}\left(k,\theta\right)\right|^2. \tag{11}$$

However, the optimization problem in (11) is over parameterized essentially, because the beamsteering structure proposed in Fig. 2 selects three types of system errors to describe all the possible distortions in steerable parametric loudspeakers. In generally, (11) is not able to solve directly. It is noted that the spacing distortion factors and the weight distortion factors are independent of the frequency, and the phase distortion factors are related with frequency. Thus, the frequency-dependent and frequency-independent factors have to be solved separately.

In Fig. 5, we introduce a combined optimization approach of the Monte Carlo method and nonlinear least squares method. First, an initial estimation of the spacing distortion factors and the weight distortion factors are generated from random vector generator with uniform distribution between 0.85 and 1.15. This range is determined from the simulation results in Fig. 3 and our past experience in measurements. Second, based on the group of randomly generated trial spacing distortion factors and weight distortion factors, the phase distortion factors can be solved by the nonlinear least squares method. Peak signal to noise ratio (PSNR) is used to evaluate the mismatch between theoretical and measured beampatterns. The measured beampatterns are considered as the original signal, and the theoretical beampatterns (before or after calibration) as the noisy approximation of the original signal. Thus, the differences between the measured beampatterns and the theoretical beampatterns are treated as noisy signals. To

improve the PSNR values, i.e. to get a more accurate estimation of the measured beampatterns, the calibration procedure is done iteratively as a training process of the proposed beamsteering structure. More iteration of trials for randomly generated weight distortion factors and spacing distortion factors are apparently required. The iteration only terminates when the overall PSNR value has not improved in the latest million iterations.

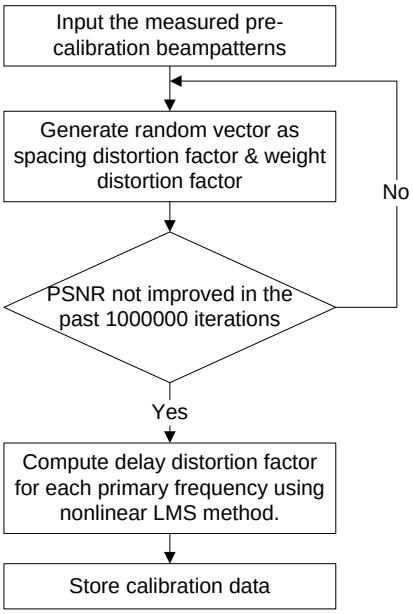

Figure 5. The flow chart for the combined optimization approach of the Monte Carlo method and nonlinear least squares method.

4. Measurement results

The primary-frequency and difference-frequency beampatterns were measured in anechoic chamber with a dimension of 6 m × 3 m × 3 m. The primary-frequency waves were captured by an 1/8 inch microphone (B&K 4138), while the difference-frequency waves were measured using a 1/2 inch microphone (B&K 4134). The ultrasonic transducer array was configured in 8 columns with 4 ultrasonic sensors (Murata MA40S4S) in each column, as shown in Fig. 6. The diameter of each ultrasonic sensor is 0.99 cm. The ultrasonic transducer array was mounted on a motorized rotation stage, and the microphones were placed at a location 4 meters away from the center of the ultrasonic transducer array. All channels in the ultrasonic transducer

array were equally weighted, but differently delayed to achieve beamsteering. The beamsteering algorithm was carried out in an 8-channel analog output board (NI PCI-6733).

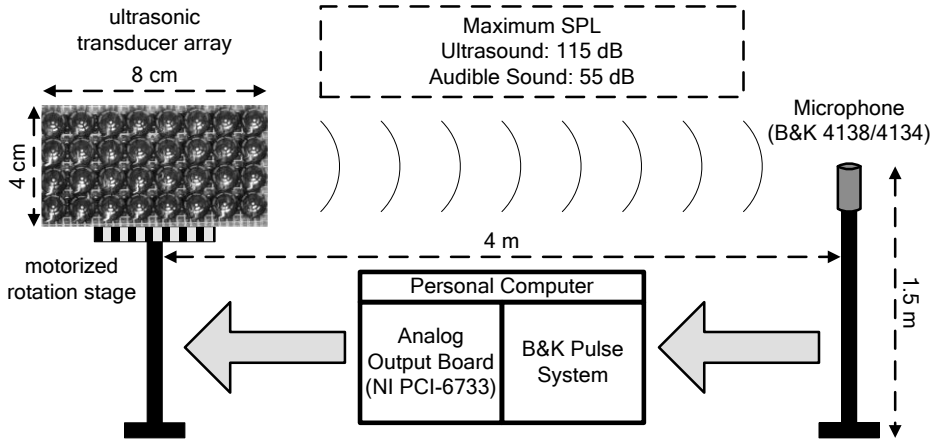

Figure 6. The experimental setup of the steerable parametric loudspeaker in anechoic chamber.

The maximum sound pressure level measured at the primary frequency and the difference frequency were 115 dB and 55 dB, respectively. The primary-frequency and difference-frequency beampatterns were measured within a restricted angle between -45˚ to 45˚ with a resolution of 1˚. The primary-frequency beampatterns are measured at 36 kHz, 38 kHz, 39 kHz, 39.5 kHz, 39.75 kHz, 40.25 kHz, 40.5 kHz, 41 kHz, 42 kHz, and 44 kHz. Thus, the difference-frequency beampatterns were measured correspondingly at 0.5 kHz, 1 kHz, 2 kHz, 4 kHz, and 8 kHz. For each primary-frequency and difference-frequency waves, the mainlobe was steered to 0°, 10° and 20°. The proposed calibration algorithm was applied to the measured primary-frequency beampatterns for all the frequencies, except at 39 kHz and 41 kHz. The calibration data of our experimental setup is listed in Table 1.

Table 1. The calibration data of the experimental setup of the steerable parametric loudspeaker.

channel no.		1	2	3	4	5	6	7	8
weight distortion factor		0.0167	0.1407	0.1376	-0.1313	-0.1285	-0.0685	-0.0536	-0.0474
spacing distortion factor		-0.0004	-0.0619	0.0288	0.0738	0.0091	0.0036	0.0725	0.0230
delay distortion factor	36 kHz	-0.0190	-0.0714	-0.0332	-0.1500	-0.1500	0.1338	0.0725	0.0086
	38 kHz	0.0045	-0.0714	0.0117	-0.1379	-0.1395	0.0226	0.0514	-0.0090
	39.5 kHz	0.0176	-0.0035	-0.0021	0.0508	0.0630	-0.0447	0.0255	-0.0280
	39.75 kHz	0.0226	-0.0320	0.1284	0.0164	0.1416	-0.0838	0.0098	-0.0099

	40.25 kHz	0.0433	0.0139	0.1121	0.1500	0.1500	-0.1073	-0.0116	-0.0301
	40.5 kHz	0.0238	0.0024	0.1143	0.0274	0.1344	-0.0748	0.0077	0.0042
	42 kHz	0.0120	-0.0162	0.0048	0.1100	0.0800	0.0924	0.0347	-0.0115
	44 kHz	0.0166	-0.0327	-0.0103	0.0749	0.0163	0.0026	-0.0164	-0.0162
(curve	39 kHz	0.0176	-0.0239	0.0607	-0.0294	0.0107	-0.0505	0.0271	-0.0192
fitting)	41 kHz	0.0304	-0.0216	0.0744	0.1235	0.1748	-0.0564	-0.0026	-0.0046

The delay distortion factor at 39 kHz and 41 kHz, which is listed in the last two rows of Table 1, are obtained from polynomial curve fitting based on the calibration data at the other primary frequencies. By applying the calibration data, the calibrated primary-frequency beampatterns at 39 kHz and 41 kHz are obtained for cross-validation. The calibrated beampatterns are compared with measured beampatterns and uncalibrated beampatterns in Fig. 7. It is shown in Figs. 7(a) and 7(b) that after calibration, the matching is improved significantly for both the grating lobe and sidelobes. Furthermore, the generated difference-frequency wave at 2 kHz is compared with the beampattern derived from the product directivity principle and the modified product directivity principle. In both Figs 7(c) and 7(d), due to the improvement of accuracy in predicting the locations of grating lobes at the primary frequency after calibration, the amplitude of grating lobe at the difference frequency is more accurately predicted as well. Moreover, the modified product directivity principle shows a better performance in matching the beamwidth of the mainlobe and the grating lobe. Through this cross validation procedure, our proposed calibration method has been proved to be practically effective for solving the system error problem in steerable parametric loudspeakers.

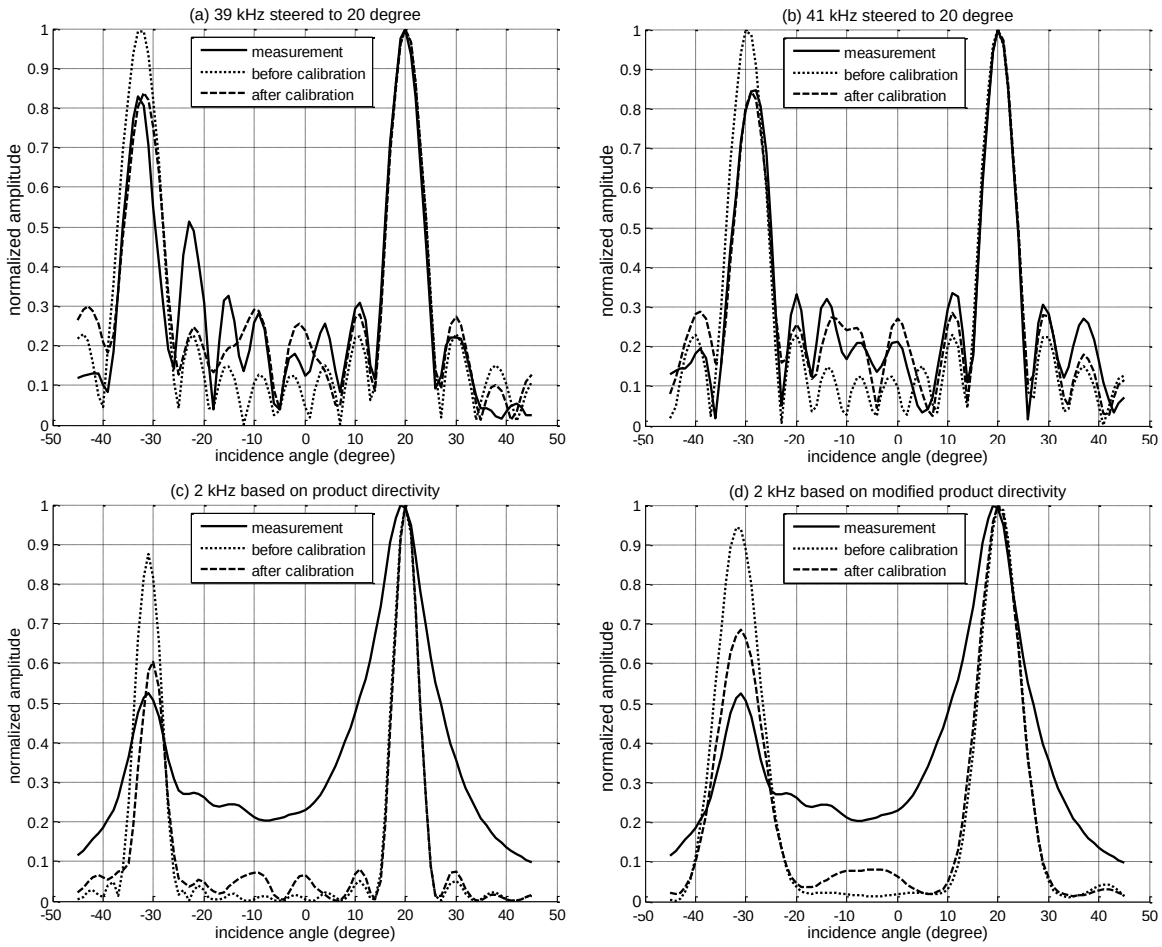

Figure 7. The comparison of beampatterns obtained from measurement and simulations (before and after calibration) for (a) the lower primary frequency is 39 kHz; (b) the higher primary frequency is 41 kHz; (c) the difference frequency is 2 kHz, and simulations are based on the product directivity principle; (d) the same difference frequency is 2 kHz, and simulations are based on modified product directivity. In all the figures, the mainlobes are steered to 20°.

A complete comparison of PSNR values before and after calibration is illustrated in Figs. 8(a) and 8(c) for the primary-frequency beampatterns, and in Figs. 8(b) and 8(d) for the difference-frequency beampatterns based on the modified product directivity principle. The overall PSNR value of the primary-frequency beampatterns is 19.72 dB; while after calibration, this value has been improved to 22.37. As noted in Fig. 8(c), when the primary-frequency wave at 38 kHz and steered to 0°, the PSNR value drops after calibration. This is due to our proposed calibration method, which is based on global optimization and result in positive PSNR improvement in most cases, as shown in Figs 8(c) and 8(d).

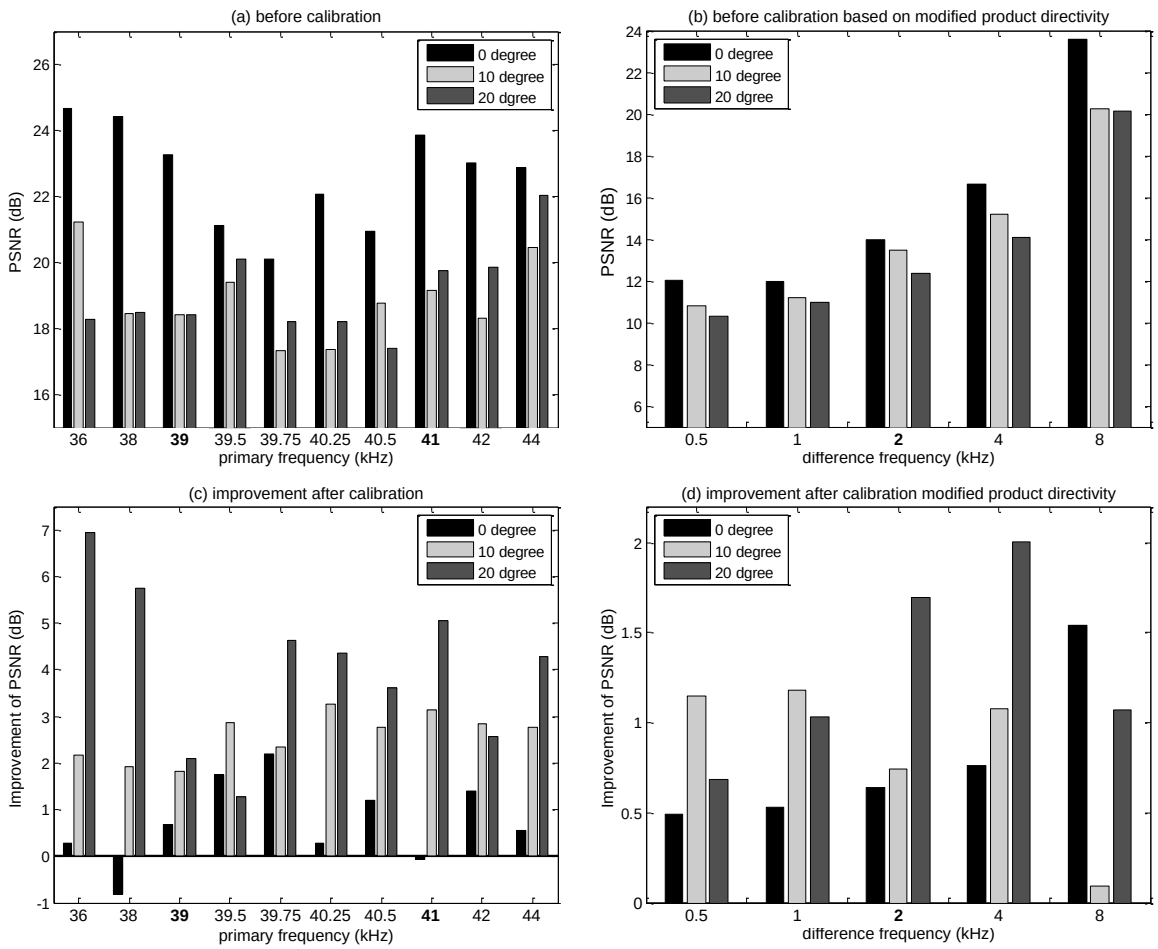

Figure 8. The PSNR values before calibration for (a) the primary-frequency beampatterns and (b) the difference-frequency beampatterns based on the modified product directivity principle. The improvement of PSNR values after calibration for (c) the primary-frequency beampatterns and (d) the difference-frequency beampatterns.

5. Conclusion

In this paper, we analyzed the degraded beampatterns caused by four types of system errors, and proposed a beamsteering structure of steerable parametric loudspeakers that takes the system errors into account. Based on the proposed beamsteering structure and the measured primary-frequency beampatterns, a combination of Monte Carlo and nonlinear least squares optimization method was applied to solve the calibration equation of steerable parametric loudspeakers. The cross-validation results show significant improvements in matching the primary-frequency beampatterns obtained from simulations and measurements. For the

difference-frequency waves, where acoustical model error is dominating, the performance of the proposed calibration approach is limited by the accuracy of product directivity principle. However, the location of grating lobe can be estimated more accurately after calibration, which is of importance to ensure better grating lobe elimination in the design of steerable parametric loudspeakers.

Acknowledge

This work is supported by the Singapore Ministry of Education Academic Research Fund Tier-2, under research grant MOE2010-T2-2-040.

References

[1] P. J. Westervelt, “Parametric acoustic array,” J. Acoust. Soc. Am., vol. 35, no. 4, pp. 535-537, 1963.

[2] M. B. Bennett and D. T. Blackstock, “Parametric array in air,” J. Acoust. Soc. Am., vol. 57, no. 3, pp. 562-568, 1975.

[3] M. Yoneyama, J. Fujimoto, Y. Kawamo, and S. Sasabe “The audio spotlight: An application of nonlinear interaction of sound waves to a new type of loudspeaker design,” J. Acoust. Soc. Am., vol. 73, no. 5, pp. 1532-1536, 1983.

[4] W. S. Gan, E. L. Tan and S. M. Kuo, “Audio Projection: Directional sound and its application in immersive communication,” IEEE Signal Processing Mag., vol. 28, no. 1, pp. 53-57, 2011.

[5] D. Olszewski, F. Prasetyo, and K. Linhard, “Steerable highly directional audio beam loudspeaker”, in Proc. Interspeech, 2005.

[6] W. S. Gan, J. Yang, K. S. Tan, and M. H. Er, “A digital beamsteerer for difference frequency in parametric array”, IEEE Trans. Audio Speech Lang. Process., vol. 14, no. 3, pp. 1018-1025, May 2006.

[7] N. Tanaka and M. Tanaka, “Active noise control using a steerable parametric array loudspeaker,” J. Acoust. Soc. Am., vol. 127, no. 6, pp. 3526-3537, 2010.

[8] C. M. Darvennes and M. F. Hamilton, “Scattering of sound by sound from two Gaussian beams,” J. Acoust. Soc. Am., vol. 87, no. 5, pp. 1955-1964, 1990.

[9] T. G. Muir and J. G. Willette, “Parametric acoustic transmitting arrays,” J. Acoust. Soc. Am., vol. 52, no. 5, pp. 1481-1486, 1972.

[10] C. Shi and W. S. Gan, “Grating lobe elimination in steerable parametric loudspeaker,” IEEE Trans. Ultrason. Ferroelectr. Freq. Control, vol. 58, no. 2, pp. 437-450, 2011.

[11] J. Berntsen, J. N. Tjotta and S. Tjotta, “Intersection of sound waves. Part IV: Scattering of sound by sound,” J. Acoust. Soc. Am., vol. 86, no. 5, pp. 1968-1983, 1989.

[12] D. H. Johnson and D. E. Dudgeon, “Array Signal Processing: Concepts and Techniques,” Prentice Hall, USA, 1993.

[13] Murata Manufacturing Co. Ltd., Ultrasonic Sensor Application Manual, Oct. 31, 2008. [Online]. Available: http://www.murata.com/products/catalog/pdf/s15e.pdf. [Accessed Jan. 13, 2012].

[14] Nippon Ceramic Co. Ltd., Parametric Speaker, [Online]. Avaiable: http://www.nicera.co.jp/pro/ut/ut-04e.html. [Accessed Jan. 13, 2012].